Icarus 225 (2013) 342–351

Contents lists available at SciVerse ScienceDirect

Icarus

journal homepage: www.elsevier.com/locate/icarus

Sulfite–sulfide–sulfate–carbonate equilibria with applications to Mars

G.M. Marion [a,*], J.S. Kargel [b], J.K. Crowley [c], D.C. Catling [d]

[a] Desert Research Institute, 2215 Raggio Parkway, Reno, NV 89512, USA
[b] Department of Hydrology & Water Resources, University of Arizona, Tucson, AZ 85721, USA
[c] P.O. Box 344, Lovettsville, VA 20180, USA
[d] Department of Earth & Space Sciences, University of Washington, Seattle, WA 98195, USA

ARTICLE INFO

Article history:
Received 13 November 2012
Revised 11 February 2013
Accepted 17 February 2013
Available online 9 April 2013

Keywords:
Mineralogy
Volcanism
Mars, Surface
Geological processes

ABSTRACT

Mars volcanic SO_2 and H_2S gas emissions are likely the dominant source of martian sulfate, and the source of sulfuric acid. Until this work, the FREZCHEM model lacked SO_2 and H_2S gases and associated sulfite and sulfide minerals. The specific objectives of this paper were to add these components and associated sulfite and sulfide minerals and phases into FREZCHEM, and to explore some possible roles of these chemistries on Mars. New solid phases added included the sulfites: $Na_2SO_3{\cdot}7H_2O$, K_2SO_3, $(NH_4)_2SO_3{\cdot}H_2O$, $MgSO_3{\cdot}6H_2O$, $CaSO_3{\cdot}0.5H_2O$, and $FeSO_3{\cdot}1.5H_2O$, and the sulfide: FeS_2. The lowest eutectic of these minerals was K_2SO_3 (= 6.57 m) at 228 K. Because sulfurous acid is stronger than carbonic acid, this causes a much larger fraction of S(IV) to exist as sulfite (SO_3^{2-}) at acidic to mildly alkaline pH, whereas almost none of the C is present as carbonate anion. Model calculations show that small quantities of SO_2 in an early CO_2-rich martian atmosphere suppressed formation of carbonates because SO_2 is much more water soluble than CO_2 and a stronger acid, which may be a major reason why sulfates are much more common than carbonates on Mars. Also, perhaps equally important are low temperatures that favor sulfite mineral precipitation, the oxidation of which leads to sulfate minerals. Another potentially important factor that favors sulfite/sulfide mineral formation is low pH values that cannot allow carbonate minerals, but can allow sulfide minerals such as pyrite (FeS_2). The presence of pyrite, highly insoluble, would lead to sulfate minerals when oxygen becomes available in acidic environments. Major cations for both sulfites (or sulfates) and carbonates (Ca and Mg) can limit carbonates. Sulfite–sulfide volcanism on a cold, lower pH, Mars are the primary causes of high sulfate minerals (e.g., Ca and Mg sulfates), compared to volcanism on a warm, higher pH, Earth that led to more abundant carbonate minerals (e.g., Ca and Mg carbonates).

1. Introduction

Mars volcanic SO_2 and H_2S gas emissions, that may have been more abundant on Mars than on Earth, have been implicated during early martian global change (Halevy et al., 2007; Bibring et al., 2008; Johnson et al., 2008; Halevy and Schrag, 2009), as the dominant source of martian sulfate (Banin et al., 1997; Bishop et al., 2004; Zolotov and Shock, 2005; Bibring et al., 2008; Halevy and Schrag, 2009), and the source of sulfuric acid (Settle, 1979; Banin et al., 1997; Papike et al., 2006; Bullock and Moore, 2007; Berger et al., 2008; Johnson et al., 2008; Halevy and Schrag, 2009). Heavy impact bombardment and the intense volcanic activity associated with that early period on Mars also may have released sulfur gases from the crust, for instance, due to thermal destabilization of ice (in permafrost) and pyrite (in volcanic rocks or carbonaceous shales), or of sulfate salts.

As a source of sulfate (including sulfate salts and sulfuric acid), SO_2 and H_2S require oxidation reactions (e.g., $H_2S + 2O_2 \iff H_2SO_4$) (Papike et al., 2006). These reactions occur in the atmosphere (Settle, 1979), even under weakly reducing and anoxic conditions characteristic of a volcanically active early Mars (Zahnle and Haberle, 2007). Formation of sulfuric acid may also occur by aqueously mediated oxidation of sulfide minerals (e.g., $FeS_2 + H_2O + 1.5O_2 \iff H_2SO_4 + Fe^{2+}$) (Bishop et al., 2004; Zolotov and Shock, 2005). Impact and magmatic heat may have contributed to oxygen release from ice or groundwater and oxidation of crustal sulfides or through dissolution of minerals such as rhomboclase ($Fe_2(SO_4)_3 \cdot H_2SO_4 \cdot 8H_2O \iff H_2SO_4 + 2Fe^{3+} + 3SO_4^{2-} + 8H_2O$) and other ferric sulfates (Marion et al., 2008). Precipitation of minerals such as ferric oxide/hydroxides through freezing or evaporation can also lead to soil acidification ($Fe_2O_3 + 6H^+ \iff 2Fe^{3+} + 3H_2O$) (McArthur et al., 1991; Lacelle et al., 2008; Marion et al., 2008) as can precipitation of minerals such as zeolites ($CaAl_2Si_4O_{12} \cdot 4H_2O + 8H^+ \iff Ca^{2+} + 2Al^{3+} + 4Si(OH)_4^0$). Sulfate salts, such as gypsum and epsomite, then can form by sulfuric acid neutralization reactions with Ca–Mg-rich silicate rocks. Kargel

* Corresponding author.
E-mail address: giles.marion@dri.edu (G.M. Marion).

0019-1035/$ - see front matter © 2013 Elsevier Inc. All rights reserved.
http://dx.doi.org/10.1016/j.icarus.2013.02.035

et al. (1999) described a wide range of both biological and abiotic routes by which elemental sulfur (not treated in this paper) is produced in mainly hydrothermal settings. They also reviewed and produced new ideas on how Jupiter's anhydrous moon, Io, may have generated copious amounts of native sulfur, SO_2, and other sulfur oxides. Another Jovian moon—Europa—has an ice-covered ocean and abundant sulfates salts and/or sulfuric acid; Kargel et al. (2000) described how either biological activity or abiotic aqueous chemistry involving SO_2 emissions into the ocean could have produced sulfates. Any of these processes potentially could have been active on Mars, where, instead of an ocean, there exists a thick icy cryosphere. The conversion of SO_2 and H_2S to sulfate are complicated (e.g., kinetics with multiple subspecies that are not treated in our model); but instead we are focused on chemical equilibrium that deals directly with sulfite, sulfide, or sulfate. Implicit in our calculations is that if sulfite or sulfide precipitates in the presence of oxygen, then sulfates will form.

On Earth, strong volcanic volatile acids include sulfuric, hydrochloric, and nitric (Banin et al., 1997); rarely or more sparingly, phosphoric acid, boric acid, and hydrobromic acid also are known in igneous and hydrothermal systems. Hydrofluoric acid also is significant in some cases of pegmatite-forming hydrothermal systems. Ubiquitous weak acids include silicic and carbonic. Hydrochloric acid has been implicated as a potential source of chloride and acidity on Mars (Keller et al., 2007). What controls sulfate and chloride concentrations, and past/current acidity on Mars is published (e.g., Fairen et al., 2004; Hurowitz et al., 2010). However, fundamentally it is the composition of igneous rocks that drives the pH of aqueous systems that equilibrate with those rocks; whether rocks are alkaline or silicic depends on things like the degree of partial melting and the activities of H_2O and CO_2. High mantle CO_2:H_2O coupled with low degrees of partial melting cause alkaline magmas to form, whereas high H_2O:CO_2 produces silicic, acidic rocks. The pathways of aqueous chemical weathering and brine evolution depend on the initial rock compositions as well as access of carbon dioxide from the atmosphere or other sources. Also, the hypothesis that sulfur gases may have contributed to the early greenhouse effect (Halevy et al., 2007; Halevy and Schrag, 2009) lacks a consensus because the photochemical residence time of SO_2 and H_2S and the albedo cooling due to sulfate aerosol clouds remain to be properly investigated; nevertheless, any large and sudden emission of SO_2 into the atmosphere of Mars due to a massive, brief eruption or large impact is expected to have a large, if geologically transient, climatic effect either to warmer or colder (possibly, first warmer and then colder) atmospheres (Halevy and Head, 2012).

Previously, the FREZCHEM model (Marion and Kargel, 2008) lacked SO_2 and H_2S gases and associated sulfite and sulfide minerals and phases. The specific objectives of this paper were to (1) add SO_2 and H_2S gases and associated sulfite and sulfide minerals into FREZCHEM, and (2) explore the role of these chemistries on Mars.

2. Methods and materials

2.1. FREZCHEM model

FREZCHEM is an equilibrium chemical thermodynamic model parameterized for concentrated electrolyte solutions (to ionic strengths = 20 molal) using the Pitzer approach (Pitzer, 1991, 1995) for the temperature range from −100 to 25 °C (CHEMCHAU version has temperature range from 0 to 100 °C) and the pressure range from 1 to 1000 bars (Marion and Farren, 1999; Marion, 2001, 2002; Marion et al., 2003, 2005, 2006, 2008, 2009a, 2009b, 2010a, 2010b, 2011, 2012; Marion and Kargel, 2008). The current version of the model is parameterized for the Na–K–NH_4–Mg–Ca–Fe(II)–Fe(III)–Al–H–Cl–ClO_4–Br–SO_4–NO_3–OH–HCO_3–CO_3–CO_2–O_2–CH_4–NH_3–Si–H_2O system; it includes 108 solid phases, including ice, 16 chloride minerals, 36 sulfate minerals, 16 carbonate minerals, five solid-phase acids, four nitrate minerals, seven perchlorates, six acid-salts, five iron oxide/hydroxides, four aluminum hydroxides, two silica minerals, two ammonia minerals, two gas hydrates, and two bromide sinks. (See above references for the model parameters.) An objective of this work was to develop sulfite–sulfide mineral parameterizations based on classical chemical thermodynamic principles that can be incorporated seamlessly into FREZCHEM. This involved the incorporation of seven new sulfite–sulfide solid phases into FREZCHEM. A FORTRAN version of the resulting model will be available from the senior author (giles.marion@dri.edu) or from http://frezchem.dri.edu after this paper is published.

2.2. Pitzer approach

In the Pitzer approach (Pitzer, 1991, 1995), the activity coefficients (γ) as a function of temperature at 1.01 bar pressure for cations (M), anions (X), and neutral aqueous species (N), such as CO_2(aq) or CH_4(aq), are given by

$$\begin{aligned}\ln(\gamma_M) = {} & z_M^2 F + \sum m_a(2B_{Ma} + ZC_{Ma}) + \sum m_c(2\Phi_{Mc} \\ & + \sum m_a \Psi_{Mca}) + \sum\sum m_a m_{a'} \Psi_{Maa'} \\ & + z_M \sum\sum m_c m_a C_{ca} + 2\sum m_n \lambda_{nM} \\ & + \sum\sum m_n m_a \zeta_{nMA} \end{aligned} \quad (1)$$

$$\begin{aligned}\ln(\gamma_X) = {} & z_X^2 F + \sum m_c(2B_{cX} + ZC_{cX}) + \sum m_a(2\Phi_{Xa} \\ & + \sum m_c \Psi_{cXa}) + \sum\sum m_c m_{c'} \Psi_{cc'X} \\ & + |z_X| \sum\sum m_c m_a C_{ca} + 2\sum m_n \lambda_{nX} \\ & + \sum\sum m_n m_c \zeta_{ncX} \end{aligned} \quad (2)$$

$$\ln(\gamma_N) = \sum m_c(2\lambda_{Nc}) + \sum m_a(2\lambda_{Na}) + \sum\sum m_c m_a \zeta_{Nca} \quad (3)$$

where B, C, Φ, Ψ, λ and ζ are Pitzer-equation interaction parameters, m_i is the molal concentration, and F and Z are equation functions. In these equations, the Pitzer interaction parameters and the F function are temperature dependent. The subscripts c, a, and n refer to cations, anions, and neutral species, respectively. The subscripts c' and a' refer to cations and anions, respectively, that differ from c and a. The activity of water (a_w) at 1.01 bar pressure is given by

$$a_w = \exp\left(\frac{-\phi \sum m_i}{55.50844}\right) \quad (4)$$

where ϕ is the osmotic coefficient, which is given by

$$\begin{aligned}(\phi - 1) = {} & \frac{2}{\sum m_i}\left\{\frac{-A_\phi I^{3/2}}{1 + bI^{1/2}} + \sum\sum m_c m_a (B_{ca}^{\phi} + ZC_{ca}) + \sum\sum m_c m_{c'} (\Phi_{cc'}^{\phi} \right. \\ & + \sum m_a \Psi_{cc'a}) + \sum\sum m_a m_{a'} (\Phi_{aa'}^{\phi} + \sum m_c \Psi_{caa'}) \\ & \left. + \sum\sum m_n m_c \lambda_{nc} + \sum\sum m_n m_a \lambda_{na} + \sum\sum\sum m_n m_c m_a \zeta_{n,c,a}\right\} \end{aligned} \quad (5)$$

The binary B parameters in Eqs. (1), (2) and (5), are functions of $B_{ca}^{(0)}$, $B_{ca}^{(1)}$ and $B_{ca}^{(2)}$ (Table 1). Similarly, the C parameters in these equations are a function of C_{ca}^{ϕ} (Table 1).

The temperature dependencies of Pitzer parameters (discussed above) and solubility products (discussed below) are defined by

$$P(T) = a_1 + a_2 T + a_3 T^2 + a_4 T^3 + a_5/T + a_6 \ln(T) \quad (6)$$

where $P(T)$ is the Pitzer parameter (Table 1) or $\ln(K_{sp})$ (Table 2) and T is absolute temperature (K); exceptions to these equations are footnoted in tables or discussed in the text.

Table 1
Binary Pitzer-equation parameters (a_1–a_3, Eq. (6)) derived in this work or taken from the literature (numbers are in computer scientific notation where $e \pm xx$ stands for $10^{\pm xx}$).

Pitzer-equation parameters	a_1	a_2	a_3	Temperature range (K)	Data sources
$B^{(0)}_{Na,HSO_3}$	0.0249			298–328	Rosenblatt (1981)
$B^{(1)}_{Na,HSO_3}$	0.2455			298–328	Rosenblatt (1981)
C^{ϕ}_{Na,HSO_3}	4.00e−4			298–328	Rosenblatt (1981)
$B^{(0)}_{Na,SO_3}$	−8.06e−2	3.407e−4		269–298	Rosenblatt (1981) and Masson et al. (1986), this work
$B^{(1)}_{Na,SO_3}$	4.778e0	−1.267e−2		269–298	Rosenblatt (1981) and Masson et al. (1986), this work
C^{ϕ}_{Na,SO_3}	0.00			269–298	Rosenblatt (1981) and Masson et al. (1986), this work
$B^{(0)}_{K,HSO_3}$	−0.096			298–328	Rosenblatt (1981)
$B^{(1)}_{K,HSO_3}$	0.2481			298–328	Rosenblatt (1981)
C^{ϕ}_{K,HSO_3}	0.00			298–328	Rosenblatt (1981)
$B^{(0)}_{K,SO_3}$	4.50e−1	−1.291e−3		228–298	Rosenblatt (1981) and Linke (1965), this work
$B^{(1)}_{K,SO_3}$	1.954e0	−3.200e−3		228–298	Rosenblatt (1981) and Linke (1965), this work
C^{ϕ}_{K,SO_3}	−3.20e−2	1.077e−4		228–298	Rosenblatt (1981) and Linke (1965), this work
$B^{(0)}_{NH_4,HSO_3}$	−0.096			298	This work[a]
$B^{(1)}_{NH_4,HSO_3}$	0.2481			298	This work[a]
$C^{\phi}_{NH_4,HSO_3}$	0.00			298	This work[a]
$B^{(0)}_{NH_4,SO_3}$	5.072e−2	−3.90e−5		260–303	Linke (1965), this work[b]
$B^{(1)}_{NH_4,SO_3}$	−4.440e−1	3.703e−3		260–303	Linke (1965), this work[b]
$C^{\phi}_{NH_4,SO_3}$	−7.842e−3	2.49e−5		260–303	Linke (1965), this work[b]
$B^{(0)}_{Mg,HSO_3}$	0.490			298–328	Rosenblatt (1981)
$B^{(1)}_{Mg,HSO_3}$	1.804			298–328	Rosenblatt (1981)
C^{ϕ}_{Mg,HSO_3}	0.00			298–328	Rosenblatt (1981)
$B^{(0)}_{Mg,SO_3}$	0.200			273–298	Rosenblatt (1981)
$B^{(1)}_{Mg,SO_3}$	3.659	−2.21e−3		273–298	Rosenblatt (1981) and Linke (1965), this work.
$B^{(2)}_{Mg,SO_3}$	−41.0			273–298	Rosenblatt (1981)
C^{ϕ}_{Mg,SO_3}	0.00			273–298	Rosenblatt (1981)
$B^{(0)}_{Ca,HSO_3}$	0.438			298–328	Rosenblatt (1981)
$B^{(1)}_{Ca,HSO_3}$	1.76			298–328	Rosenblatt (1981)
C^{ϕ}_{Ca,HSO_3}	0.00			298–328	Rosenblatt (1981)
$B^{(0)}_{Ca,SO_3}$	0.200			298	Rai et al. (1991)
$B^{(1)}_{Ca,SO_3}$	3.1973			298	Rai et al. (1991)
$B^{(2)}_{Ca,SO_3}$	−133.6			298	Rai et al. (1991)
C^{ϕ}_{Ca,SO_3}	0.00			298	Rai et al. (1991)
$\overline{V}^{(0)}_{so_3}$	8.278112e4	−8.910971e2	3.195979e0[c]	273–303	Linke (1965), this work
$K^{(0)}_{SO_3}$	0.00				This work

[a] Assumed the same as K,HSO_3.
[b] Assumed parameters for $NH_4,SO_3 = NH_4,SO_4$ at 298 K that were extended to lower temperatures using ice data (see Fig. 3).
[c] This equation also contains: $-3.819702e{-}3 * T^3$.

Table 2
Equilibrium constants (as $\ln(K)$) (a_1–a_3, Eq. (6)) derived in this study (numbers are in computer scientific notation where $e \pm xx$ stands for $10^{\pm xx}$).

Solution-solid phase equilibria	a_1	a_2	a_3	Solid phase molar volumes (cm^3/mol)[a]	Temperature range (K)	References
$Na_2SO_3 \cdot 7H_2O \iff 2Na^+ + SO_3^{2-} + 7H_2O$	−2.217911e1	1.075468e−1	−1.398402e−4	163.84	269–298	Masson et al. (1986), this work
$K_2SO_3 \iff 2K^+ + SO_3^{2-}$	5.891507e0	1.989583e−2	−1.065820e−4	(62.63)	227–303	Linke (1965), this work
$(NH_4)_2SO_3 \cdot H_2O \iff 2NH_4^+ + SO_3^{2-} + H_2O$	−6.890744e0	2.249496e−2		95.14	260–303	Linke (1965), this work
$MgSO_3 \cdot 6H_2O \iff Mg^{2+} + SO_3^{2-} + 6H_2O$	−2.471916e1	8.390197e−2	−1.024246e−4	123.17	273–308	Linke (1965) and Nyvlt (2001), this work
$CaSO_3 \cdot 0.5H_2O \iff Ca^{2+} + SO_3^{2+} + 0.5H_2O$	−11.4443	−1.2896e−2		51.25	273–298	Rai et al. (1991) and Pasiuk-Bronikowska and Rudzinski (1990), this work
$FeSO_3 \cdot 1.5H_2O \iff Fe^{2+} + SO_3^{2-} + 1.5H_2O$	−13.3855			(108.49)	293	Masson et al. (1986), this work
$H^+ + FeS_2 \iff Fe^{2+} + HS^- + S_0$	−37.7624			24.00	298	Morse et al. (1987)
$HS^- \iff H^+ + S^{2-}$	−31.7296				298	Morse et al. (1987)

[a] Solid phase molar volumes are calculated by $V_m = M/\rho$, where M is molar mass and ρ is density. Values in parentheses are approximated by comparisons to sulfate cases.

FREZCHEM specifies the density and pressure dependence of equilibrium constants (K), activity coefficients (γ), and the activity of water (a_w). An example is how density is calculated with the equation

$$\rho = \frac{1000 + \sum m_i M_i}{\frac{1000}{\rho^0} + \sum m_i \overline{V}_i^0 + V_{mix}^{ex}} \quad (7)$$

where m_i is the molal concentration, M_i is the molar mass, ρ^0 is the density of pure water at a given temperature and pressure, $\overline{V}_i^0$ is the partial molar volume at infinite dilution of solution species, and V_{mix}^{ex} is the excess volume of mixing given by

$$V_{mix}^{ex} = A_v \left(\frac{I}{b}\right) \ln(1 + bI^{0.5}) + 2RT \times \sum\sum m_c m_a \left[B_{c,a}^{v} + \left(\sum m_c z_c\right) C_{c,a}^{v}\right] \quad (8)$$

where A_v is the volumetric Pitzer–Debye–Hückel parameter, I is the ionic strength, b is a constant (1.2 $kg^{0.5}$ $mol^{-0.5}$), and $B_{c,a}^{v}$ and $C_{c,a}^{v}$ are functions of $B_{ca}^{(0)v}$, $B_{ca}^{(1)v}$ and $B_{ca}^{(2)v}$ and $C_{c,a}^{v}$. See Marion et al. (2005), Marion and Kargel (2008), or Marion et al. (2008) for a complete description of these density–pressure equations.

3. Results

3.1. Pitzer parameterization and solubility products

In this section, we present tables and figures that contain new equations relevant to sulfur gases (SO_2 and H_2S), and sulfite and sulfide chemistries. See earlier papers cited in Section 2.1 that document the range of previously published chemistry equations. A substantial fraction of the parameterizations for FREZCHEM rely on data in Linke (1965) and Masson et al. (1986), largely because they compiled data sets that include chemistries at subzero temperatures as required for FREZCHEM.

The Pitzer parameters for the Na–SO_3 interactions at 298.15 were taken from Rosenblatt (1981). These parameters were extended to lower temperatures by fitting to $(Na)_2SO_3$-ice data from Masson et al. (1986) (Fig. 1) using the equation

$$P(T) = P(298.15) + A(298.15 - T) \quad (9)$$

where $P(T)$ is the Pitzer parameter, T is temperature, and A is a derived constant. Knowing the freezing point depression of a solution in equilibrium with pure ice (Fig. 1) allows one to directly determine the activity of water (a_w) and the solution osmotic coefficient (ϕ, Eq. (4)), which then can serve as the thermodynamic foundation for estimating the value of Pitzer parameters (Eq. (5)) at subzero temperatures. While Eq. (9) was used to estimate the temperature dependence, this equation was converted to our standard format (Eq. (6)) in Table 1. Parameterization of Na–SO_3 interaction parameters to 270 K (Fig. 1) allowed us to estimate the equilibrium constant for $(Na)_2SO_3{\cdot}7H_2O$ (Table 2) based on solubility data (Masson et al., 1986). The model-calculated eutectic for this system occurred at 269.58 K with $(Na)_2SO_3$ = 0.982 m, which is in good agreement with the literature values of 269.71 K with $(Na)_2SO_3$ = 0.948 m (Fig. 1) (Masson et al., 1986).

The Pitzer parameters for K–SO_3 interactions at 298.15 K were taken from Rosenblatt (1981), and extended to lower temperatures with K_2SO_3-ice data from Linke (1965) (Fig. 2, Table 1). Parameterization of the ice line to 228 K allowed us to estimate the equilibrium constant for K_2SO_3 (Table 2). The solubility product of K_2SO_3 at the eutectic was model calculated at 228.45 K with K_2SO_3 = 6.56 m, which is in reasonable agreement with the literature values of 227.65 K at 6.58 m (Fig. 2) (Linke, 1965). K_2SO_3 (Fig. 2) is much more soluble than either $(Na)_2SO_3{\cdot}7H_2O$ (Fig. 1) or $(NH_4)_2SO_3{\cdot}H_2O$ (Fig. 3).

The Pitzer parameters for NH_4–SO_3 interactions at 298.15 were assumed equal to NH_4–SO_4, and extended to lower temperatures with $(NH_4)_2SO_3$-ice data from Linke (1965) (Fig. 3, Table 1). Parameterization of the ice line to 260 K allowed us to estimate the equilibrium constant for $(NH_4)_2SO_3{\cdot}H_2O$ (Table 2). The solubility product of $(NH_4)_2SO_3{\cdot}H_2O$ at the eutectic was model calculated at 260.25 K with $(NH_4)_2SO_3{\cdot}H_2O$ = 3.49 m, which is in excellent agreement with the literature values of 260.19 K with $(NH_4)_2SO_3{\cdot}H_2O$ = 3.49 m (Fig. 3) (Linke, 1965).

The Pitzer parameters for Mg–SO_3 interactions at 298.15 K were taken from Rosenblatt (1981), and extended to lower temperatures with $MgSO_3$ data from Linke (1965) (Fig. 4, Table 1). Several data sets, including those taken from Linke (1965) and Masson et al. (1986), place $MgSO_3$ in close plots at lower temperatures (273–303 K) (Nyvlt, 2001). The eutectic in this case occurred at 273.07 K with $MgSO_3$ = 0.03245 m, which is close to the lowest literature value of 273.15 K at 0.03249 m (Fig. 4). Of the four sulfites so far examined (Figs. 1–4), $MgSO_3$ is relatively insoluble.

We were only able to obtain two data points for $CaSO_3$ at low temperatures (273 and 298 K). The Pitzer parameters (Table 1)

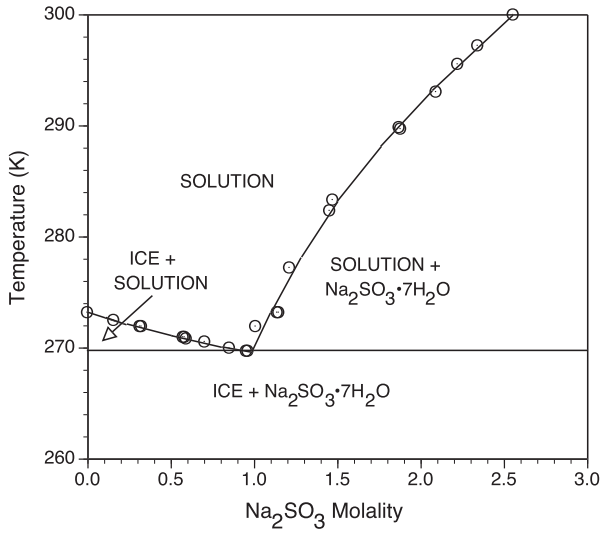

Fig. 1. Equilibrium of sodium sulfite in the 270–300 K temperature range. Symbols are experimental data; solid lines are model estimates.

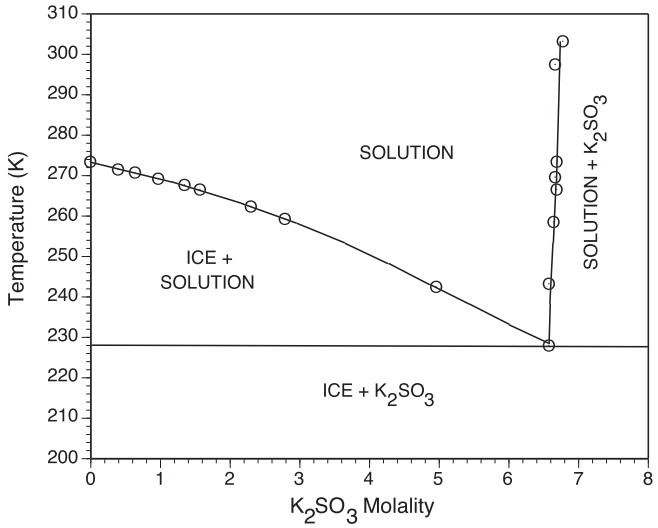

Fig. 2. Equilibrium of potassium sulfite in the 228–303 K temperature range. Symbols are experimental data; solid lines are model estimates.

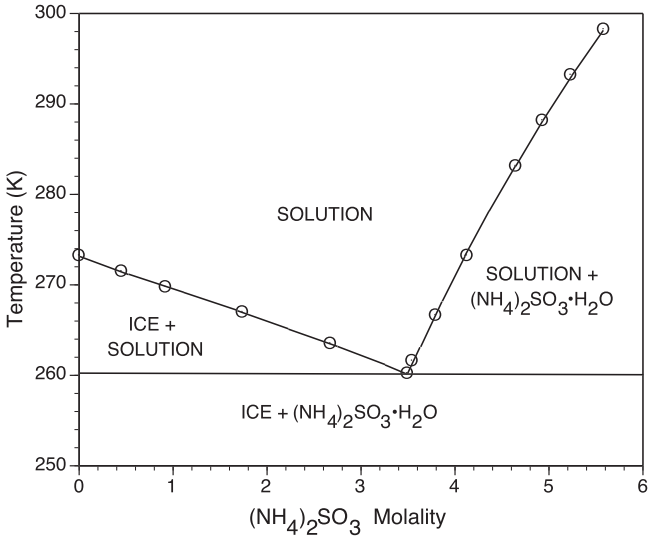

Fig. 3. Equilibrium of ammonium sulfite in the 260–298 K temperature range. Symbols are experimental data; solid lines are model estimates.

and equilibrium constant (Table 2) for $CaSO_3{\cdot}0.5H_2O$ at 298 K were taken from Rai et al. (1991). An equilibrium constant at 273 K was taken from Pasiuk-Bronikowska and Rudzinski (1990). We fit a straight-line equation for $CaSO_3{\cdot}0.5H_2O$ (Table 2) to these two data points. The equation leads to a slightly increasing $CaSO_3{\cdot}0.5H_2O$ solubility at lower temperatures, which agrees with the 303–373 K solubility of $CaSO_3{\cdot}0.5H_2O$ (Masson et al., 1986). The calculated eutectic in this case occurred at 273.15 with $CaSO_3$ = 0.00081 m, which is even more insoluble than $MgSO_3$ (see last paragraph).

We estimated the activity product of $FeSO_3{\cdot}1.5H_2O$ based on a single solubility case at 293 K from Masson et al. (1986) (Table 2). A marked difference between monovalent cations (Na, K, NH_4, Figs. 1–3, Table 2) and divalent cations (Mg, Ca, Fe, Fig. 4, Table 2) are much lower solubilities of divalent cations compared to monovalent cations (compare Figs. 1–4).

The equilibrium constant for pyrite (FeS_2) and $HS^- – S^{2-}$ equilibrium at 298 K (Table 2) were taken from Morse et al. (1987). A third equilibrium constant from Morse et al. (1987) represents

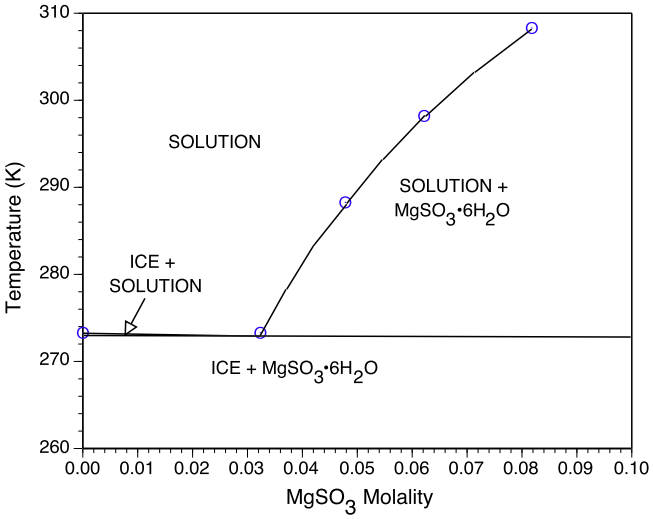

Fig. 4. Equilibrium of magnesium sulfite in the 273–308 K temperature range. Symbols are experimental data; solid lines are model estimates.

$$H_2S^0 \iff H^+ + HS^- \tag{10}$$

with the equilibrium constant equal to

$$\mathrm{Log}_{10}(K) = -32.55 - 1519.44/T + 15.672 * \log_{10}(T) - 0.02772 * T \tag{11}$$

We also took three equilibriums from Goldberg and Parker (1985) that are temperature dependent for the reactions

$$SO_2^0(aq) + H_2O(l) \iff H^+(\mathrm{aq}) + HSO_3^-\mathrm{aq} \tag{12}$$

where the equilibrium constant is

$$R\ln K = \frac{-10,600}{298.15} - 17,800\left[\frac{1}{298.15} - \frac{1}{T}\right] - 272\left[\left(\frac{298.15}{T}\right) - 1 + \ln\left(\frac{T}{298.15}\right)\right] + \frac{298.2}{2} \times (1.7)\left[\left(\frac{T}{298.15}\right) - \left(\frac{298.15}{T}\right) - 2\ln\left(\frac{T}{298.15}\right)\right] \tag{13}$$

with R = 8.31441 J K^{-1} mol^{-1}; then

$$HSO_3^-(\mathrm{aq}) \iff H^+(\mathrm{aq}) + SO_3^{2-}(aq) \tag{14}$$

where the equilibrium constant is

$$R\ln K = \frac{-40,940}{298.15} - 3650\left[\frac{1}{298.15} - \frac{1}{T}\right] - 262\left[\left(\frac{298.15}{T}\right) - 1 + \ln\left(\frac{T}{298.15}\right)\right] + \frac{298.15}{2} \times (-2.7)\left[\left(\frac{T}{298.15}\right) - \left(\frac{298.15}{T}\right) - 2\ln\left(\frac{T}{298.15}\right)\right] \tag{15}$$

and finally,

$$SO_2(\mathrm{g}) \iff SO_2^0(\mathrm{aq}) \tag{16}$$

where the equilibrium constant is

$$R\ln k = \frac{510}{298.15} - 26,970\left[\frac{1}{298.15} - \frac{1}{T}\right] + 155\left[\left(\frac{298.15}{T}\right) - 1 + \ln\left(\frac{T}{298.15}\right)\right] + \frac{298.15}{2} \times (-0.035)\left[\left(\frac{T}{298.15}\right) - \left(\frac{298.15}{T}\right) - 2\ln\left(\frac{T}{298.15}\right)\right] \tag{17}$$

The last equilibrium constant added to this model was also a Henry's law equation

$$H_2S(\mathrm{g}) \iff H_2S(\mathrm{aq}) \tag{18}$$

where the equilibrium constant is

$$K_H = 55.5\exp((4134 - 26.9 * T)/(RT)) \tag{19}$$

that was taken from De Bruyn et al. (1995) with R = 1.98722 cal K^{-1} mol^{-1}. The equilibrium constant in this case is in mol l^{-1} atm^{-1} (activity coefficients were not used). We converted this equation to mol $kg(H_2O)^{-1}$ bar^{-1} (K_H^*) for FREZCHEM by converting with

$$K_H^* = K_H(1/1.01325) * (\mathrm{SOLN}/\rho) \tag{20}$$

where ρ = density (kg(soln.)/l) and SOLN is kg(soln.)/kg(H_2O) calculated by

$$\mathrm{SOLN} = 1.00 + S_A/1000 \tag{21}$$

with

$$S_A = \sum m_i wt_i \tag{22}$$

where S_A is the absolute salinity (g salt/kg(H_2O)) with m_i = molality and wt_i = g salt/mole. See Marion (2007) for a more complete description of this conversion technique.

The Na–, K–, NH_4–, and Mg–SO_3 data allowed us to estimate binary parameters (Table 1) and equilibrium constants (Table 2) across a temperature range to their eutectics (Figs. 1–4). The other binary parameters were largely limited to 298–328 K based on Rosenblatt (1981) (Table 1). There are a few cases in Tables 1 and 2 that are based on surrogates. For example, $B^0_{NH_4,\ HSO_3} = B^0_{K,\ HSO_3}$, and $B^0_{NH_4,\ SO_3} = B^0_{NH_4,\ SO_4}$ (Table 1). Binary neutral species such as CO_2(aq), O_2(aq), SO_2(aq), and H_2S(aq) with cations (or anions) were based on surrogates (e.g., $\lambda_{Na,SO2} = \lambda_{Na,CO2}$, $\lambda_{Cl,SO2} = \lambda_{Cl,CO2}$, $\lambda_{Na,H2S} = \lambda_{Na,O2}$, $\lambda_{Cl,H2S} = \lambda_{Cl,O2}$, etc.). The data defining the CO_2(aq) and O_2(aq) cases are in Marion and Kargel (2008). We have also used surrogates for HS^- and S^{2-}. For example, $B^{(0)}_{Na,HS^-} = B^{(0)}_{Na,HSO_4^-}$, $B^{(0)-}_{NaS^{2-}} = B^{(0)}_{NaSO_4^{2-}}$ Similar examples for $B^{(1)}_{ca}$, $B^{(2)}_{ca}$, and C^{ϕ}_{ca} were used for Na, K, Ca, Mg, H, Fe(II), and NH_4. The HSO_4^- and SO_4^{2-} are all listed in Marion and Kargel (2008) and Marion et al. (2012). Surrogates were widely used for other multiple parameters that are unlisted. For example, volumetric parameters used in Eqs. (7) and (8) (B^v and C^v) were all surrogates. For Na, we set $B^{v(0)}_{Na,HSO_3} = B^{v(0)}_{Na,HSO_4}$, $B^{v(0)}_{Na,SO_3} = B^{v(0)}_{Na,SO_4}$, $B^{v(0)}_{Na,HS} = B^{v(0)}_{Na,HSO_4}$, $B^{v(0)}_{Na,S} = B^{v(0)}_{Na,SO_4}$, and similarly for K, Ca, Mg, H, Fe(II), and NH_4.

4. Validations and limitations

While model fits to experimental data are encouraging and point out the self-consistency of the model and data inputs (Figs. 1–4), they are not validations, which require comparison to independent data for multi-component solutions. Unfortunately, there are not a lot of independent data for most of the cases we summarized in Tables 1 and 2 and Figs. 1–4. An exception was the data sets for $MgSO_3$ summarized in Nyvlt (2001) that demonstrated very similar concentration–temperature plots. But in multiple cases in Tables 1 and 2, we were only capable of defining parameters and equilibrium constants at 298 K. Also, in the last paragraph, there were multiple surrogates for many cases. As a consequence, there are significant limitations to the validity of these sulfur gas and sulfite and sulfide chemistries. Nevertheless, the model provides estimates that are available at present, which will be demonstrated in applications to Mars.

FREZCHEM is an equilibrium chemical thermodynamic model as previously discussed (Section 2.1). The model as structured cannot deal directly with kinetics. But, the FREZCHEM model can be used to compare with kinetics that could illuminate chemistries on Earth, Mars, and other cold Solar System bodies.

FREZCHEM to date has included the following gases: CO_2, O_2, CH_4, NH_3, SO_2, and H_2S. But the criteria by which these gases are inputted into FREZCHEM are not all the same. For example, CO_2(input) = f(CO_2(g) + carbonate alkalinity), O_2(input) = f(O_2(g)), CH_4(input) = f(CH_4(g)), NH_3(input) = f(NH_3(g)) or f(NH_3(aq)), SO_2(input) = f(sulfite alkalinity), and H_2S(input) = f(sulfide alkalinity). The "alkalinity" terms refer to: (1) ($HCO_3^- + 2CO_3^{2-}$), (2) ($HSO_3^- + 2SO_3^{2-}$), and (3) ($HS^- + 2S^{2-}$). Inputs of O_2(g) and CH_4(g) will lead to model-calculated O_2(aq) and CH_4(aq). Inputs of sulfite alkalinity and sulfide alkalinity will lead to model-calculated SO_2(g) and H_2S(g). These alternative approaches were chosen for convenience; that is, it is sometimes easier to know the gas or solution concentrations; but one can reverse inputs indirectly if needed. For example, if you want a case where pSO_2 (partial pressure) = 1.0 bars, then substitute sulfite alkalinity values until a specific sulfite alkalinity leads to a calculated pSO_2 = 1.0 bars.

5. Applications to planetary environments

In the next four figures, the logarithmic term will be presented as log (to the base 10), which is easier to visualize compared to the ln (natural logarithm) version used in our models (e.g., Table 2).

Fig. 5 illustrates the distribution of aqueous sulfite (SO_2, HSO_3^-, SO_3^{2-}), sulfide (H_2S, HS^-, S^{2-}), sulfate (HSO_4^-, SO_4^{2-}), and carbonic (CO_2, HCO_3^-, CO_3^{2-}) species over the pH range from 0 to 11. Standout differences among sulfite, sulfide, sulfates and carbonic species are evident. For example, between pH 3.0 and 6.0, the dominant sulfite species is HSO_3^-, the dominant sulfide species is H_2S^0, the dominant sulfate species is SO_4^{2-}, and the dominant carbonic species is CO_2^0. Between pH 7 and 10, the dominant sulfite species is SO_3^{2-}, the dominant sulfide species is HS^-, the dominant sulfate species is SO_4^{2-} and the dominant carbonic species is HCO_3^-. As has been long known, and as FREZCHEM also shows, the ionic compositions of sulfite, sulfide, sulfate, and carbonic species are highly pH dependent. Below, we will illustrate both pH and temperature dependence at cryogenic conditions for systems of broad interest to aqueous geochemistry on Mars and other cold, icy realms of the Solar System.

Fig. 6 illustrates the temperature dependence of CO_2 and SO_2 Henry's law constants, Ca and Mg carbonates, and Ca and Mg sulfites. The CO_2 and SO_2 Henry's law constants increase as temperature declines. The $MgCO_3$ mineral increases in solution concentration as temperature declines, as do $CaCO_3$ and $CaSO_3{\cdot}0.5H_2O$ but only at lower rates. On the other hand, $MgSO_3{\cdot}6H_2O$ is more soluble at high temperatures but decreases in solution concentration as temperature declines. These equilibrium patterns can influence distribution of minerals, as we will illustrate next.

Fig. 5 clearly shows differences in the distribution of aqueous sulfite, sulfide, sulfate, and carbon ions. But also important are differences among SO_2, H_2S, and CO_2 gas distributions. In our Ca simulation (Fig. 7), the model inputs were NaCl = 5.0 m, Ca = 0.1 m, carbonate alkalinity ($HCO_3^- + 2CO_3^{2-}$) = 0.1 equivalents kg(H_2O)$^{-1}$, sulfite alkalinity ($HSO_3^- + 2SO_3^{2-}$) = 0.1 equivalents kg(H_2O)$^{-1}$ and pCO_2 = 0.0001 bars. Similarly, the inputs for the Mg case (Fig. 7) were NaCl = 5.00, Mg = 0.25 m, carbonate alkalinity = 0.1 equivalents kg(H_2O)$^{-1}$, sulfite alkalinity = 0.40 equivalents kg(H_2O)$^{-1}$ and pCO_2 = 0.0001 bars. In both these cases, pSO_2 was calculated from sulfite alkalinity. The high concentrations of NaCl were used to prevent ice formation at T = 253–273 K. The choices of other constituents were to force simultaneous precipitation of the carbonate and sulfite minerals (e.g., $CaCO_3 = CaSO_3{\cdot}0.5H_2O$, $MgCO_3 = MgSO_3{\cdot}6H_2O$). This allows a comparison of equilibrium along a temperature dependence (Fig. 7). Halevy et al. (2007) demonstrated how the solubility of sulfite and carbonate minerals differed at 298 K; for example, $CaSO_3{\cdot}0.5H_2O = CaCO_3$ where $\log(pSO_2/pCO_2) = -7.31$. Running FREZCHEM model for similar chemistries led to $CaSO_3{\cdot}0.5H_2O = CaCO_3$ at $\log(pSO_2/pCO_2) = -7.33$ at 298 K (Fig. 7), in excellent agreement with the Halevy et al. model. If the pSO_2 value becomes higher than the value at 298 K (pSO_2 = 4.7e−12 bars) (Fig. 7, the blue line), or pCO_2 becomes lower than the value at 298 K (pCO_2 = 1.0e−4 bars), then $CaSO_3{\cdot}0.5\ H_2O$ becomes the dominant solid phase, and if pSO_2 becomes lower or pCO_2 becomes higher, then $CaCO_3$ becomes the dominant phase. Despite the much lower pSO_2 value (4.7e−12 bars) compared to the pCO_2 (1.0e−4 bars), the SO_3^{2-} aqueous value (0.0053 m) is higher than the CO_3^{2-} aqueous value (0.000033 m) because SO_2 is much more water soluble than CO_2 and SO_3^{2-} is more pH-dependent than CO_3^{2-} (Fig. 5).

The "blue line"[1] ($CaCO_3 = CaSO_3{\cdot}0.5H_2O$) and "green line" ($MgCO_3 = MgSO_3{\cdot}6H_2O$) (Fig. 7) decrease with decreasing tempera-

[1] For interpretation of color in Fig. 7, the reader is referred to the web version of this article.

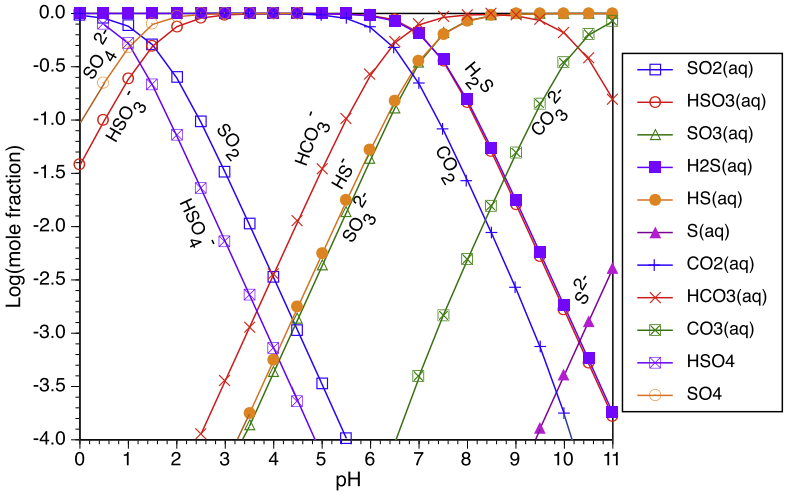

Fig. 5. The relative distribution of aqueous sulfite, sulfide, sulfate, and carbonate ions and neutrals in the pH range from 0 to 11.

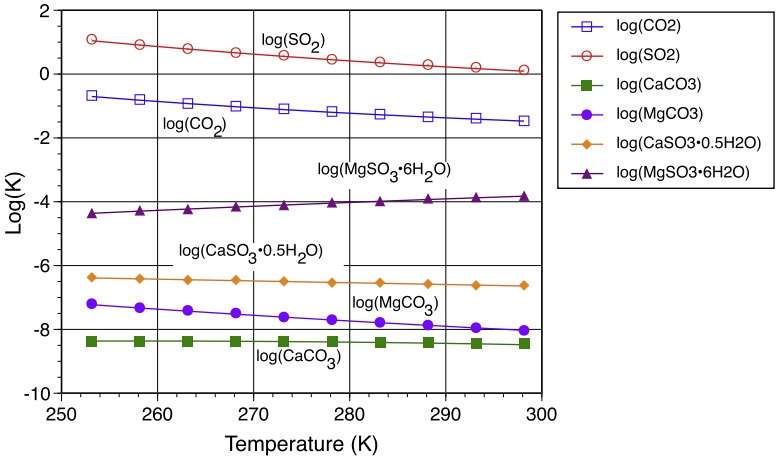

Fig. 6. Equilibrium constants for Henry's law constants, carbonate minerals, and sulfite minerals.

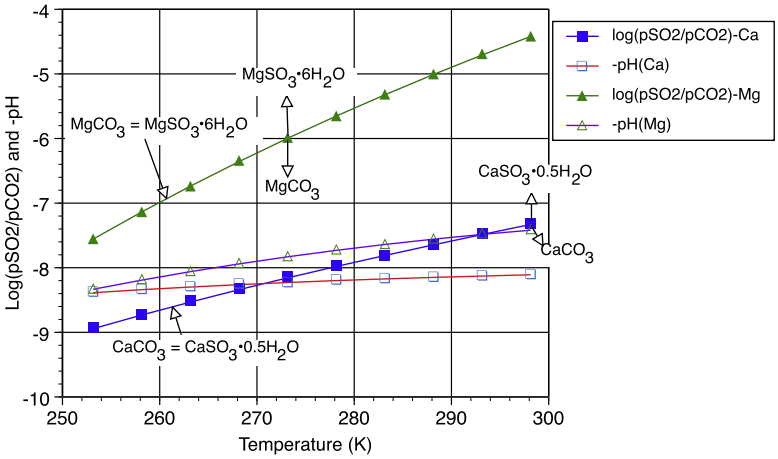

Fig. 7. The distribution of Ca and Mg carbonate and sulfite minerals as functions of pCO_2 and pSO_2 gas concentrations and temperatures.

ture, which is due to the higher solubility of $CaCO_3$ and $MgCO_3$ at low temperatures, and the lower solubility of $MgSO_3{\cdot}6H_2O$ and a very small increase of $CaSO_3{\cdot}0.5H_2O$ at low temperatures (Fig. 6). At least for these Ca and Mg minerals over the 253–298 K temperature range, lower temperatures favor higher precipitation of the sulfite minerals.

In the Ca simulation, we arbitrarily assigned $pCO_2 = 0.0001$ bars, which led to a pH range of 8.11–8.39. Assigning $pCO_2 = 1.0$ bars, for the Ca case, led to pH = 5.90–5.94, which led to $CaCO_3 = CaSO_3{\cdot}0.5H_2O$ that is identical to Fig. 7, except for the pH values that were much lower. Similar results occurred for the Mg case, except

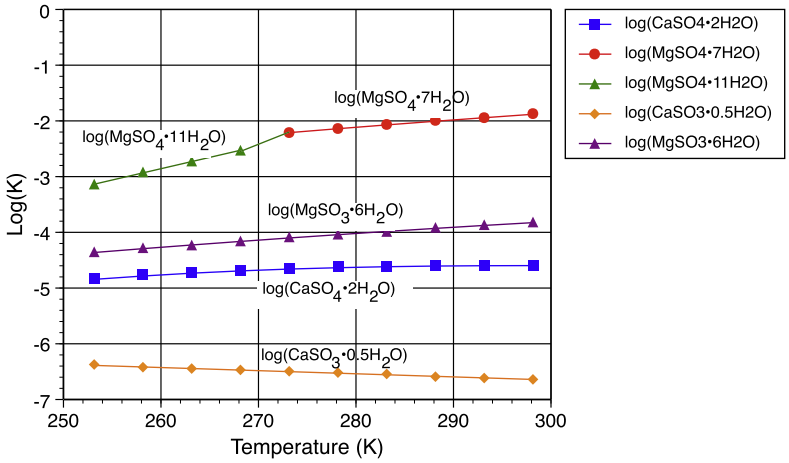

Fig. 8. Equilibrium constants for sulfate and sulfite minerals.

that the pH values were slightly different from the Ca cases. So pCO_2, per se, did not strongly influence sulfite/carbonate equilibrium. Note that sulfites can prevent formation of carbonates under both acidic and alkaline pH values, which agrees with Halevy et al. (2007) and Halevy and Schrag (2009).

Fig. 7 shows how carbonates and sulfites (and subsequently sulfates) might have formed on Mars under alkaline environments with pH values in the 7.5–8.5 range. A classic example is the Phoenix Mission that had soils that were dominated by carbonates, sulfates, and perchlorates (Catling et al., 2009; Fisher et al., 2009; Hecht et al., 2009; Kounaves et al., 2009; Marion et al., 2010a), but there are many areas on Mars that led to mineral formation under strongly acidic environments such as Meridiani Planum (e.g., Morris et al., 2006; Squyres et al., 2006). Such diverse assemblages of salts show that Mars, like Earth, has a complex history resulting in heterogeneous chemistries.

What role, if any, would sulfites and sulfides play in acidic environments? Fig. 8 depicts equilibrium constants of $MgSO_3$, $MgSO_4$, $CaSO_3$, and $CaSO_4$ (Marion and Kargel, 2008; Table 2). Now if pH was high such as in Fig. 7, then the less soluble SO_3^{2-} compared to SO_4^{2-} would be favored. For example, we ran a simulation with concentrations equal to Ca = 0.1 m, Mg = 1.0 m, Cl = 1.0 m, SO_4 = 0.4 m, and sulfite alkalinity = 0.4 equiv. $kg(H_2O)^{-1}$ over the temperature range of 273–298 K with pH controlled by sulfite alkalinity. In this case, the pH values were in the range of 7.44–7.62, and only $CaSO_3{\cdot}0.5H_2O$ and $MgSO_3{\cdot}6H_2O$ precipitated. But we also ran a similar case at a fixed pH = 3.0 that only resulted in sulfate precipitation ($CaSO_4{\cdot}2H_2O$). And the reason for sulfate and no sulfite is simply due to the dominant role of SO_4^{2-} at pH = 3.0 and very little SO_3^{2-} at this pH (see Fig. 5). Oxygen and acidic environments favor sulfate precipitation.

But, there is at least one exception dealing with Fe(II) and sulfide ions that can lead to precipitation of FeS_2(pyrite). Note how insoluble pyrite is in Table 2. We ran several pH cases from ≈0 to 7.4 with Fe^{2+}, H_2S, and a few other constituents such as Mg^{2+}, Cl^-, and SO_4^{2-}. At every pH value, Fe^{2+} adsorbed virtually all sulfide ions because pyrite is highly insoluble. A potential reaction that is not in FREZCHEM (today) is the interaction between oxygen and pyrite that would convert pyrite sulfides into sulfates that are characteristic of acidic environments such as Rio Tinto in Spain (Hubbard et al., 2009) and Meridiani Planum on Mars (Zolotov and Shock, 2005). Our simple explanation (oxygen and pyrite) cannot cope with the many elements that form between our initial components and sulfate. Nevertheless, if atmospheric oxygen were present in acidic environments, then virtually all pyrite sulfides would be converted into sulfates that are realistic for real cases on Earth and Mars (Zolotov and Shock, 2005; Hubbard et al., 2009).

6. Discussion

Our primary focus was on sulfites and sulfides as these new additions to the FREZCHEM model were relevant to Mars. But on Mars today, sulfur is largely present as sulfates (e.g., gypsum, kieserite, "polyhydrates"), at least on the surface. There is abundant evidence that sulfites and sulfides on Mars converted to sulfates both in the atmosphere and on the surface (Settle, 1979; Bishop et al., 2004; Zolotov and Shock, 2005; Zahnle and Haberle, 2007; Gaillard and Scaillet, 2009; Tian et al., 2010). SO_2 may have provided warming on a wet early Mars (Halevy et al., 2007; Halevy and Schrag, 2009); but, warming would have been offset within months by cooling from sulfate and sulfur aerosols on early Mars (Tian et al., 2010). That being the case, cold temperatures might also have played a major role in sulfite/sulfide conversion to sulfate mineralization on Mars (Fig. 7).

Despite an early CO_2-rich atmosphere on Mars, a number of authors (Halevy et al., 2007; Zahnle and Haberle, 2007; Johnson et al., 2008; Gaillard and Scaillet, 2009; Halevy and Schrag, 2009; Tian et al., 2010) attributed the prevalence of sulfur in martian surfaces as due to the role of SO_2 and H_2S gases, which is a result consistent with our model (Fig. 7). In a wet environment with free O_2, conversions from sulfite/sulfide to sulfates would be rapid. There is evidence for this process in recent papers (e.g., Halevy and Schrag, 2009; Chevrier et al., 2012). Small quantities of SO_2 in a CO_2-rich atmosphere suppress formation of carbonates (Fig. 7), which may be a major reason why sulfates are much more common on Mars. Also, perhaps equally important is temperature that favors $CaSO_3{\cdot}0.5H_2O$ and $MgSO_3{\cdot}6H_2O$ precipitation at lower temperatures (Fig. 7). SO_2-rich volcanic emissions on Earth are associated with some andesitic volcanism and may be further related to high-temperature breakdown of sulfates; such was the case, for instance, with the El Chichón (1982) (Vedder et al., 1983) and Mount Pinatubo (1991) (Hattori, 1993; Guo et al., 2004) eruptions. SO_2-rich hydrothermal pools, such as those at Yellowstone (Stahl et al., 1985), are associated with microbial redox activity. It remains to be shown by future exploration whether microbial redox activity may have been important in the martian sulfur cycle, as on Earth, or whether pure abiogenic chemistry has controlled martian sulfur cycles. And acidic pH favors sulfates compared to carbonates, sulfites, and sulfides (except for pyrite). Sulfite–sulfide volcanism on a

cold, lower pH, Mars are the primary causes of high sulfate minerals (e.g., Ca and Mg sulfates), compared to volcanism on a warm, higher pH, Earth that led to more abundant carbonate minerals (e.g., Ca and Mg carbonates).

7. Conclusions

The main conclusions of this study were:

(1) Volcanic sulfite and sulfide gases are the likely sources of sulfates on Mars. In this study, we added sulfite and sulfide gases and minerals into the FREZCHEM model.
(2) New minerals and solid phases added included $Na_2SO_3 \cdot 7H_2O$, K_2SO_3, $(NH_4)_2SO_3 \cdot H_2O$, $MgSO_3 \cdot 6H_2O$, $CaSO_3 \cdot 0.5H_2O$, $FeSO_3 \cdot 1.5H_2O$, and FeS_2. The lowest eutectic of these minerals was K_2SO_3 (= 6.57 m) at 228 K.
(3) Small quantities of SO_2 in an early CO_2-rich martian atmosphere suppressed formation of carbonates because SO_2 is much more water soluble than CO_2 and a stronger acid (Fig. 7), which may be a major reason why sulfates are much more common on Mars.
(4) Also perhaps equally important are low temperatures that favor sulfite mineral precipitation (Fig. 7), the oxidation of which leads to the formation of sulfate minerals.
(5) Another potentially important factor that favors sulfite/sulfide mineral formation are low pH values that will not allow carbonate minerals but can allow sulfide minerals such as pyrite (FeS_2). The presence of pyrite, highly insoluble, would lead to sulfate minerals when oxygen becomes available.
(6) Sulfite–sulfide volcanism on a cold, lower pH, Mars are the primary causes of high sulfate minerals (e.g., Ca and Mg sulfates), compared to volcanism on a warm, higher pH, Earth that led to more abundant carbonate minerals (e.g., Ca and Mg carbonates).

Acknowledgments

Funding was provided by a NASA Mars Fundamental Research Program entitled "Martian Geochemical Application with FREZCHEM." We thank reviewers of this paper that enlightened the scientific cases.

References

Banin, A., Han, F.X., Kan, I., Cicelsky, A., 1997. Acidic volatiles and the Mars soil. J. Geophys. Res. 102, 13341–13356.
Berger, G., Treguier, E., d'Uston, C., Pinet, P., Toplis, M.J., 2008. The role of volcanic sour gas on the alteration of martian basalt: Insights from geochemical modeling. Lunar Planet. Sci. XXXIX. Abstract 1809.
Bibring, J.-P., Langevin, Y., Poulet, F., Gondet, B., OMEGA Science Team, 2008. Mars global history derived from OMEGA/Mars express observations. Lunar Planet. Sci. XXXIX. Abstract 2009.
Bishop, J.L., Darby Dyar, M., Lane, M.D., Banfield, J.F., 2004. Spectral identification of hydrated sulfates on Mars and comparison with acidic environments on Earth. Int. J. Astrobiol. 3, 275–285.
Bullock, M.A., Moore, J.M., 2007. Atmospheric conditions on early Mars and the missing layered carbonates. Geophys. Res. Lett. 34, L19201. http://dx.doi.org/10.1029/2007GL030688.
Catling, D.C. et al., 2009. Atmospheric origins of perchlorate on Mars and in the Atacama. J. Geophys. Res. http://dx.doi.org/10.1029/2009/JE003425.
Chevrier, V.F., Dehouck, E., Lozano, C.G., Altheide, T.S., 2012. Mineral parageneses resulting from weathering on early Mars and the effect of CO_2 vs. SO_2 atmospheres. In: Third Conf. on Early Mars, Abstract 7080.
De Bruyn, W.J. et al., 1995. Henry's law solubilities and Setchenow coefficients for biogenic reduced sulfur species obtained from gas–liquid uptake measurements. J. Geophys. Res. 100, 7245–7251.
Fairen, A.G., Fernandez-Remolar, D., Dohm, J.M., Baker, V.R., Amils, R., 2004. Inhibition of carbonate synthesis in acidic oceans on early Mars. Nature 431, 423–426.
Fisher, D.A., Hecht, M.H., Kounaves, S., Catling, D., 2009. Perchlorate found by Phoenix could provide a mobile brine sludge at the bed of Mars northern ice cap that would allow flow with very low basal temperatures: Possible mechanism for water table re-charge. Lunar Planet. Sci., Houston, TX. Abstract #2281.
Gaillard, F., Scaillet, B., 2009. The sulfur content of volcanic gases on Mars. Earth Planet. Sci. Lett. 279, 34–43.
Goldberg, R.N., Parker, V.B., 1985. Thermodynamics of solution of SO_2(g) in water and of aqueous sulfur dioxide solutions. J. Res. Nat. Bur. Stand. 90, 341–358.
Guo, S., Bluth, G.J.S., Rose, W.I., Watson, I.M., 2004. Re-evaluation of SO_2 release of the 15 June 1991 Pinatubo eruption using ultraviolet and infrared satellite sensors. Geochem. Geophys. Geosyst. 5, Q04001. http://dx.doi.org/10.1029/2003GC000654.
Halevy, I., Head III, J.W., 2012. Punctuated volcanism, transient warming and global change in the late Noachian–early Hesperion. Lunar Planet Sci. XLIII. Abstract 1908.
Halevy, I., Schrag, D.P., 2009. Sulfur dioxide inhibits calcium carbonate precipitation: Implications for early Mars and Earth. Geophys. Res. Lett. 36. http://dx.doi.org/10.1029/2009GL040792.
Halevy, I., Zuber, M.T., Schrag, D.P., 2007. A sulfur dioxide climate feedback on early Mars. Science 318, 1903–1907.
Hattori, K., 1993. High-sulfur magma, a product of fluid discharge from underlying mafic magma: Evidence from Mount Pinatubo, Philippines. Geology 21, 1083–1086.
Hecht, M.H. et al., 2009. Detection of perchlorate and the soluble chemistry of martian soil at the Phoenix lander site. Science 325, 64–67.
Hubbard, C.G., Black, S., Coleman, M.L., 2009. Aqueous geochemistry and oxygen isotope compositions of acid mine drainage from the Rio Tinto, SW Spain, highlight inconsistencies in current models. Chem. Geol. 265, 321–334.
Hurowitz, J.A., Fischer, W., Tosca, N.J., Milliken, R.E., 2010. Origin of acidic surface waters and the evolution of atmospheric chemistry on early Mars. Nat. Geosci. 3, 323–326.
Johnson, S.S., Pavlov, A.A., Mischna, M.A., 2008. Longevity of atmospheric SO_2 on early Mars. Lunar Planet. Sci. XXXIX. Abstract 2090.
Kargel, J.S., Delmelle, P., Nash, D.B., 1999. Volcanogenic sulfur on Earth and Io: Composition and spectroscopy. Icarus 142, 249–280.
Kargel, J.S., Kaye, J., Head III, J.W., Marion, G., Sassen, R., Crowley, J., Prieto, O., Grant, S., Hogenboom, D.L., 2000. Europa's crust and ocean: Origin, composition, and the prospects for life. Icarus 148, 226–265.
Keller, J.M. et al., 2007. Equatorial and mid-latitude distribution of chlorine measured by Mars Odyssey GRS. J. Geophys. Res. 111. http://dx.doi.org/10.1029/2006JE002679.
Kounaves, S.P. et al., 2009. The wet chemistry experiments on the 2007 Phoenix Mars Scout Lander Mission: Data analysis and results. J. Geophys. Res. http://dx.doi.org/10.1029/2009/JE003424.
Lacelle, D., Leveille, R., Lauriol, B., Clark, I.D., Doucet, A., 2008. Acid drainage and associated sulphate mineral formation near Eagle Plains, northern Yukon, Canada: Analogue to the Meridiani Planum sulphates on Mars. Lunar Planet. Sci. XXXIX. Abstract 1264.
Linke, W.F., 1965. Solubilities of Inorganic and Metal Organic Compounds, vol. II, 4th ed. Am. Chem. Soc., Washington, DC.
Marion, G.M., 2001. Carbonate mineral solubility at low temperatures in the Na–K–Mg–Ca–H–Cl–SO_4–OH–HCO_3–CO_3–CO_2–H_2O system. Geochim. Cosmochim. Acta 65, 1883–1896.
Marion, G.M., 2002. A molal-based model for strong acid chemistry at low temperatures (<200 to 298 K). Geochim. Cosmochim. Acta 66, 2499–2516.
Marion, G.M., 2007. Adapting molar data (without density) for molal models. Comput. Geosci. 33, 829–834.
Marion, G.M., Farren, R.E., 1999. Mineral solubilities in the Na–K–Mg–Ca–Cl–SO_4–H_2O system: A re-evaluation of the sulfate chemistry in the Spencer–Møller–Weare model. Geochim. Cosmochim. Acta 63, 1305–1318.
Marion, G.M., Kargel, J.S., 2008. Cold Aqueous Planetary Geochemistry with FREZCHEM: From Modeling to the Search for Life at the Limits. Springer, Berlin.
Marion, G.M., Catling, D.C., Kargel, J.S., 2003. Modeling aqueous ferrous iron chemistry at low temperatures with application to Mars. Geochim. Cosmochim. Acta 67, 4251–4266.
Marion, G.M., Kargel, J.S., Catling, D.C., Jakubowski, S.D., 2005. Effects of pressure on aqueous chemical equilibria at subzero temperatures with applications to Europa. Geochim. Cosmochim. Acta 69, 259–274.
Marion, G.M., Catling, D.C., Kargel, J.S., 2006. Modeling gas hydrate equilibria in electrolyte solutions. Calhad 30, 248–259.
Marion, G.M., Kargel, J.S., Catling, D.C., 2008. Modeling ferrous–ferric iron chemistry with application to martian surface geochemistry. Geochim. Cosmochim. Acta 72, 242–266.
Marion, G.M., Catling, D.C., Kargel, J.S., 2009a. Br/Cl portioning in chloride minerals in the Burns formation on Mars. Icarus 200, 436–445.
Marion, G.M. et al., 2009b. Modeling aluminum–silicon chemistries and application to Australian acidic playa lakes as analogues for Mars. Geochim. Cosmochim. Acta 73, 3493–3511.
Marion, G.M., Catling, D.C., Zahnle, K.J., Claire, M.W., 2010a. Modeling aqueous perchlorate chemistries with applications to Mars. Icarus 207, 675–685.
Marion, G.M., Mironenko, M.V., Roberts, M.W., 2010b. FREZCHEM: A geochemical model for cold aqueous solutions. Comput. Geosci. 36, 10–15.
Marion, G.M., Catling, D.C., Crowley, J.K., Kargel, J.S., 2011. Modeling hot spring chemistries with applications to martian silica formation. Icarus 212, 629–642.

Marion, G.M., Kargel, J.S., Catling, D.C., Lunine, J.I., 2012. Modeling ammonia–ammonium aqueous chemistries in the Solar System's icy bodies. Icarus 220, 932–946.
Masson, M.R., Lutz, H.D., Engelen, B., 1986. Solubility Data Series, Sulfites, Selenites, and Tellurites, vol. 26. Pergamon Press, Oxford.
McArthur, J.M., Turner, J.V., Lyons, W.B., Osborn, A.O., Thirlwall, M.F., 1991. Hydrochemistry on the Yilgarn Block, Western Australia: Ferrolysis and mineralization in acidic brines. Geochim. Cosmochim. Acta 55, 1273–1288.
Morris, R.V. et al., 2006. Mössbauer mineralogy of rock, soil, and dust at Meridiani Planum, Mars: Opportunity's journey across sulfate-rich outcrop, basaltic sand and dust and hematite lag deposits. J. Geophys. Res. 111, E12S15. http://dx.doi.org/10.1029/2006JE002791.
Morse, J.W., Millero, F.J., Cornwell, J.C., Rickard, D., 1987. The chemistry of the hydrogen sulfide and iron sulfide systems in natural waters. Earth-Sci. Rev. 24, 1–42.
Nyvlt, J., 2001. Solubilities of magnesium sulfite. J. Therm. Anal. Calorim. 66, 509–512.
Papike, J.J., Karner, J.M., Shearer, C.K., 2006. Comparative planetary mineralogy: Implications of martian and terrestrial jarosite. A crystal chemical perspective. Geochim. Cosmochim. Acta 70, 1309–1321.
Pasiuk-Bronikowska, W., Rudzinski, K.J., 1990. Rownowagowy sklad oraz pH wodnych zawiesin $CaSO_3$ i $Ca(OH)_2$ (Polish). Przem. Chem. 69, 503–506.
Pitzer, K.S., 1991. Ion interaction approach: Theory and data correlation. In: Pitzer, K.S. (Ed.), Activity Coefficients in Electrolyte Solutions, second ed. CRC Press, Boca Raton, pp. 75–153.
Pitzer, K.S., 1995. Thermodynamics, third ed. McGraw-Hill, New York.
Rai, D., Felmy, A.R., Fulton, R.W., Moore, D.A., 1991. An aqueous thermodynamic model for Ca^{2+}—SO_3^{2-} ion interactions and the solubility product of crystalline $CaSO_3{\cdot}1/2H_2O$. J. Solution Chem. 20, 623–632.
Rosenblatt, G.M., 1981. Estimation of activity coefficients in concentrated sulfite–sulfate solutions. AIChE J. 27, 619–626.
Settle, M., 1979. Formation and deposition of volcanic sulfate aerosols on Mars. J. Geophys. Res. 84, 8343–8354.
Squyres, S.W. et al., 2006. Overview of the Opportunity Mars Exploration Rover Mission to Meridiani Planum: Eagle Crater to Purgatory Ripple. J. Geophys. Res. 111, E12S12. http://dx.doi.org/10.1029/2006JE002771.
Stahl, D.A., Lane, D.J., Olsen, G.J., Pace, N.R., 1985. Characterization of a Yellowshone hot spring microbial community by 5S rRNA sequences. Appl. Environ. Microbiol. 49, 1379–1384.
Tian, F. et al., 2010. Photochemical and climate consequences of sulfur outgassing on early Mars. Earth Planet. Sci. Lett. 295, 412–418.
Vedder, J.F., Condon, E.P., Inn, E.C.Y., Tabor, K.D., Kritz, M.A., 1983. Measurements of stratospheric SO_2 after the El Chichon eruptions. Geophys. Res. Lett. 10, 1045–1048.
Zahnle, K., Haberle, R.M., 2007. Atmospheric sulfur chemistry on ancient Mars. In: Seventh Inter. Conf. Mars, Abstract 3256.
Zolotov, M.Y., Shock, E.L., 2005. Formation of jarosite-bearing deposits through aqueous oxidation of pyrite at Meridiani Planum, Mars. Geophys. Res. Lett. 32, L21203. http://dx.doi.org/10.1029/2005GL02453.